Room-Temperature Synthesis of Copper and Silver, Nanocrystalline Chalcogenides in Mixed Solvents

Yang Jiang,*,† Bo Xie,* Ji Wu,* Shengwen Yuan, Yue Wu,* Hao Huang,* and Yitai Qian*,1

*Structure Research lab and Department of Chemistry, University of Science and Technology of China, Hefei, Anhui 230026, Peoples Republic of China; and
†Institute of Material Science and Engineering, Hefei University of Technology, Hefei, Anhui 230009, People's Republic of China

Copper and silver nanocrystalline chalcogenides, $Cu_{2-x}Se$, Cu_2Te, Ag_2Se, and Ag_2Te, have been successfully synthesized in a mixture of ethylenediamine and hydrazine hydrate as a solvent at room temperature. Products showed different morphologies, such as nanotubes, nanorods, and nanoparticles. The results indicated that the coordination and chelation abilities of ethylenediamine play an important role in the formation of one-dimensional nanocrystalline binary chalcogenides, and hydrazine hydrate is crucial to the electron transfer in the room temperature reactions. These transition-metal nanocrystalline chalcogenides as prepared were analyzed by X-ray powder diffraction, transmission electron microscopy, and X-ray photoelectron spectroscopy. The UV-Vis absorption properties of these nanocrystals were also measured.   © 2002 Elsevier Science (USA)

I. INTRODUCTION

Transition-metal nanocrystalline chalcogenides have attracted much attention over the past years due to their great potential applications and their interesting properties (1–4). Among these chalcogenides, copper chalcogenides have been widely used as thermoelectric cooling materials (5, 6), optical filters (7), optical recording materials (8), solar cells (9), and superionic materials (10). The semiconducting phase of the silver chalcogenides, Ag_2S, Ag_2Se, and Ag_2Te, historically have received less attention than other semiconductors with narrow band gaps and high carrier mobilities (11). But recent experiments have revealed that these compounds have large magnetoresistive effects depending on the composition, which shows obvious technological prospects (12).

Traditionally, these transition-metal chalcogenides have been synthesized by solid-state reaction of elements (13), solid-state metathesis (14), and self-propagating high-temperature synthesis (15). These processes are usually carried out at elevated temperatures, and give little control in particle size, crystallizability, and stoichiometry of products. When gaseous H_2E ($E =$ S, Se, Te) was used to prepare chalcogenides from aqueous solutions of the metal cations, the process has been relatively dangerous and highly toxic (16). Parkin and co-workers reported a room-temperature route to Ag and Cu chalcogenides in liquid ammonia. Most of the products Parkin obtained are amorphous and usually crystallized after heat treatment at 300°C (17, 18). During Parkin's experiments, several manipulations had to be carried out very carefully at −77°C in thick-walled glass vessels. Recently, our group has successfully synthesized copper and silver chalcogenides by using solvothermal methods at temperatures in the range of 140–180°C. The products were usually formed as nanoparticles (19, 20).

In this paper, we report a room-temperature reaction to nanocrystalline copper and silver chalcogenides from redox reactions in mixture of ethylenediamine and hydrazine hydrate as a solvent, which can be considered as a convenient and soft chemical method. One interesting result is that the $Cu_{2-x}Se$ nanotube has been obtained through this procedure. Although the chalcogenides MQ_2 ($M =$ Mo, W; $Q =$ S, Se) with graphite-like layered structure are also capable of forming nanotubes or fullerene-type structure (21, 22), this cubic phase $Cu_{2-x}Se$ nanotube represents a new example of nanotubes for chalcogenides.

II. EXPERIMENTAL SECTION

All reagents were of analytic grade or better and used without further purification. Reactions were carried out at 25°C. X-ray diffraction (XRD) patterns were determined on Japan Rigaku Dmax γ-A X-ray diffractometer with graphite monochromatized Cu$K\alpha$ radiation ($\lambda = 1.5418$ Å). They were indexed using JCPDS cards. To obtain further information about stoichiometry of some compounds,

---

^{1}To whom correspondence should be addressed. Fax: +86 551 363 1760. E-mail: ytqian@ustc.edu.cn.

X-ray photoelectron spectroscope (XPS) analysis was carried out on a VGESCALAB MK II X-ray photoelectron spectrometer, using non-monochromatized Mg$K\alpha$ as the excitation source and choosing C1s (284.60 eV) as the reference line. TEM images were taken on a Hitachi model H-800 transmission electron microscope, using an accelerating voltage of 200 kV. In addition, the ultraviolet absorption spectroscope was collected with a Shimadzu UV-Vis recording spectrophotometer (UV-240).

A. Formation of $Cu_{2-x}Se$ or Cu_2Te Nanocrystallines by Room-Temperature Reaction of CuO with Se or Te Powders in the Mixed Solvent

The same reaction scale and procedure exemplified here for $Cu_{2-x}Se$ was adopted for nanocrystalline Cu_2Te.

Powdered CuO (0.796 g, 0.01 mol) and Se (0.395 g, 0.005 mol) were put into a conical flask with a capacity of 100 mL, then a mixed solvent consisting of 30 mL ethylenediamine and 15 mL hydrazine hydrate was added into the flask. The flask was maintained at room temperature with a constant electromagnetic stirring for 24 h. The mixture changed to a dark green/black color and finally to green with a black precipitate. The precipitate was collected by vacuum filtration and washed several times with hot distilled water (80°C), absolute ethanol, carbon disulfide, and absolute ethanol in that order, then vacuum dried at 70°C for 4 h. The obtained sample was analyzed by XRD, XPS, and TEM.

B. Formation of Nanocrystalline Ag_2Se or Ag_2Te by Room Temperature Reaction of AgCl with Se or Te Powder in the Mixed Solvent

The same reaction conditions and scales were used as described above for CuO except that, in the AgCl reaction, the reaction time was chosen to be about 8 h. The obtained samples were also analyzed by XRD, XPS, and TEM.
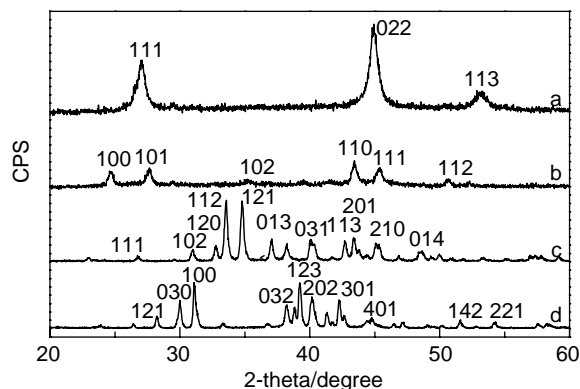

FIG. 1. XRD patterns of the samples as prepared in the mixed solvent of ethylenediamine and hydrazine hydrate at room temperature: (a) $Cu_{2-x}Se$, (b) Cu_2Te, (c) Ag_2Se, and (d) Ag_2Te.

III. RESULTS AND DISCUSSION

A. Synthesis and Characterization of Nanocrystalline $Cu_{2-x}Se$ and Cu_2Te

The XRD patterns of as-prepared samples are shown in Fig. 1. The phase and cell constants of copper and silver chalcogenides are listed in Table 1. All peaks shown in Fig. 1a can be indexed to cubic phase $Cu_{2-x}Se$, the calculated cell constant is close to the value of JCPDS 6-680, no impurity phase could be detected. Further information of $Cu_{2-x}Se$ was obtained by the X-ray photoelectron spectroscopy analysis. The binding energies of Se3d and Cu2$p3$ are 54.45 and 923.3 eV, respectively. The kinetic energy of CuL_3vv peak is 926.7 eV. Therefore, the value of the "modified Auger parameter" (α') is 1850.0 eV, which can be used to differentiate it from CuSe and Cu_2Se, and the modified Auger parameter (α') is close to that of Cu(I), this XPS feature should arise from main Cu(I) and less Cu(II) valence states (23, 24). According to

TABLE 1
Characterization of As-Prepared Products

Products	Morphology	Phase	Average size (nm)		Cell constants	
			From TEM	From XRD	Calculated	JSPDS card
$Cu_{2-x}Se$	Nanotube (main) Lamellar	Cubic	Ø30 × Ø20 × 500	32.1	$a = 5.68$ Å	$a = 5.73$ Å
Cu_2Te	Nanorod	Hexagonal	20 × 120	23.8	$a = 4.275$ Å	$a = 4.237$ Å
					$c = 7.286$ Å	$c = 7.274$ Å
Ag_2Se	Long particles	Orthorhombic	40 × 100	53.2	$a = 4.303$ Å	$a = 4.333$ Å
					$b = 7.052$ Å	$b = 7.062$ Å
					$c = 7.779$ Å	$c = 7.764$ Å
Ag_2Te	Nanorod	Monoclinc	10 × 50	11.4	$a = 8.172$ Å	$a = 8.170$ Å
					$b = 8.951$ Å	$b = 8.941$ Å
					$c = 8.069$ Å	$c = 8.065$ Å
					$\beta = 112.73°$	$\beta = 112.8°$

electroneutral rule, the ratio of Cu(I) to Cu(II) can be calculated as 90.4:9.6. Quantification of XPS survey spectrum peaks (shown in Fig. 2a) give the ratio of Cu to Se as 1.825:1. TEM image (Fig. 3a) of the $Cu_{2-x}Se$ sample shows the main morphology to be that of uniform nanotubes with open ends. The $Cu_{2-x}Se$ nanotubes have a length of 500 nm with an inner diameter of 20 nm and an outer diameter of 30 nm on average as shown in Table 1.

The XRD pattern shown in Fig. 1b can be indexed to the hexagonal phase Cu_2Te. The cell constants shown in Table 1 are close to the data of JCPDS 39-1061. XPS analysis indicated that the molar ratio of Cu to Te is 1.981:1, which is in good agreement with the stoichiometry of Cu_2Te. The TEM image (Fig. 3b) shows that the morphology of Cu_2Te to be that of nanorods with an average length of 120 nm and a diameter of 20 nm. The electron diffraction pattern (inset in Fig. 3b) taken from the selected area of the nanorods proves the presence of single-crystal Cu_2Te.

The room-temperature reaction of CuO with Se, or Te in mixed solvent of ethylenediamine and hydrazine hydrate produced nanocrystalline copper selenide and telluride in good yield. The formation of nanocrystalline copper chalcogenides results from redox reaction. In the reaction process, hydrazine hydrate also acts as a reducing agent, which is helpful to dissolve Te or Se in the mixed solvent.
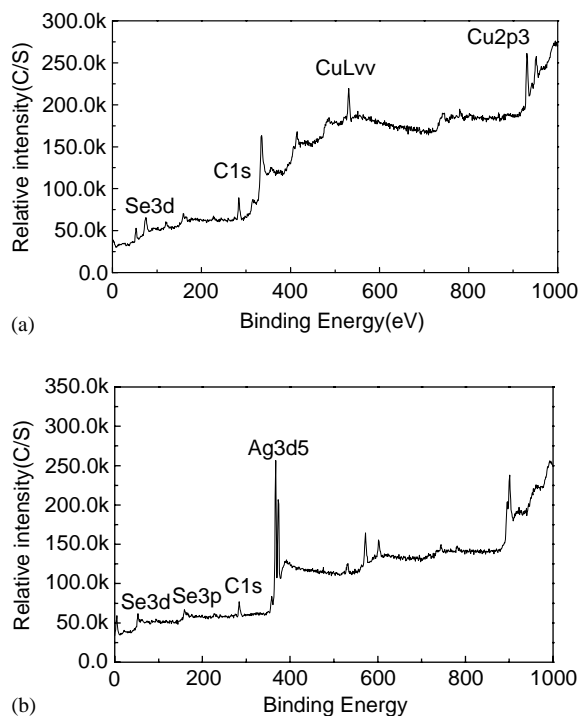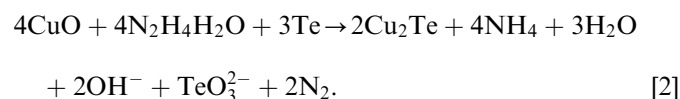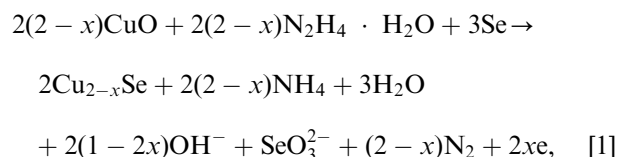
Ethylenediamine is a strongly coordinating base and has N-chelation. When Se or Te and CuO were dispersed in the alkaline mixed solvent, the disproportionation of Se or Te occurred and produced Se^{2-} and SeO_3^{2-} or Te^{2-} and TeO_3^{2-} ions, respectively (25, 26). Meanwhile, CuO could be dissolved in the mixed solvent slowly to form Cu^{2+} complex with ethylenediamine, and then partly was reduced to a Cu^+ complex by hydrazine hydrate which could react with Te^{2-} and Se^{2-} to form $Cu_{2-x}Se$ and Cu_2Te. The possible reaction procedure could be expressed as follows:

$$2(2-x)CuO + 2(2-x)N_2H_4 \cdot H_2O + 3Se \rightarrow$$

$$2Cu_{2-x}Se + 2(2-x)NH_4 + 3H_2O$$

$$+ 2(1-2x)OH^- + SeO_3^{2-} + (2-x)N_2 + 2xe, \quad [1]$$

$$4CuO + 4N_2H_4H_2O + 3Te \rightarrow 2Cu_2Te + 4NH_4 + 3H_2O$$

$$+ 2OH^- + TeO_3^{2-} + 2N_2. \quad [2]$$

Because of the strong coordinating ability and the structure of ethylenediamine, it can easily chelate Cu^{2+} and Cu^+ to form stable complexes of $[Cu(en)_2]^{2+}$ ($\beta_2 = 10^{19.99}\,M^{-2}$) and $[Cu(en)_2]^+$ ($\beta_2 = 10^{11.4}M^{-2}$); thus, it effectively slows down the formation rate of binary chalcogenides $Cu_{2-x}Se$ which may be benefit for the growth of nanotubes under the effect of structure-directing agent ethylenediamine. After the Se^{2-} anions self-organize with the complex $[Cu(en)_2]^+$ reduced from $[Cu(en)_2]^{2+}$ by hydrazine hydrate to form one-dimensional structure, the coordinated ligands are lost gradually. We assumed that this molecular template mechanism was similar to that of vanadium oxide nanotubes (V_2O_x-NTs) reported by Nesper et al. (27, 28). Like vanadium cations of V_2O_x-NTs, copper cations of $Cu_{2-x}Se$ nanotubes adopt mixed valences. Although further investigation about a reliable model for the structure and growth is in progress, we find that the $Cu_{2-x}Se$ nanocrystalline morphology is obviously influenced by the composition of the mixed solvent. The $Cu_{2-x}Se$ nanotubes were obtained at the initial volume ratio of ethylenediamine to hydrazine hydrate varying from 3 to 2, a further decrease of the molecular template (ratio less than 2) content led to the formation of $Cu_{2-x}Se$ with a lamellar morphology. For Cu_2Te, although the reaction process of CuO with Te was the same as that of CuO with Se, no Cu_2Te nanotubes were observed.

B. Synthesis and Characterization of Ag_2Se and Ag_2Te Nanocrystalline

All of the peaks of XRD pattern shown in Fig. 1c could be indexed to the orthorhombic phase Ag_2Se. The cell constants, $a = 4.303$, $b = 7.052$, and $c = 7.779$ Å calculated

FIG. 2. XPS spectra of the samples as prepared: (a) typical XPS survey spectrum of $Cu_{2-x}Se$ nanotubes and (b) typical XPS survey spectrum of Ag_2Se nanoparticles.
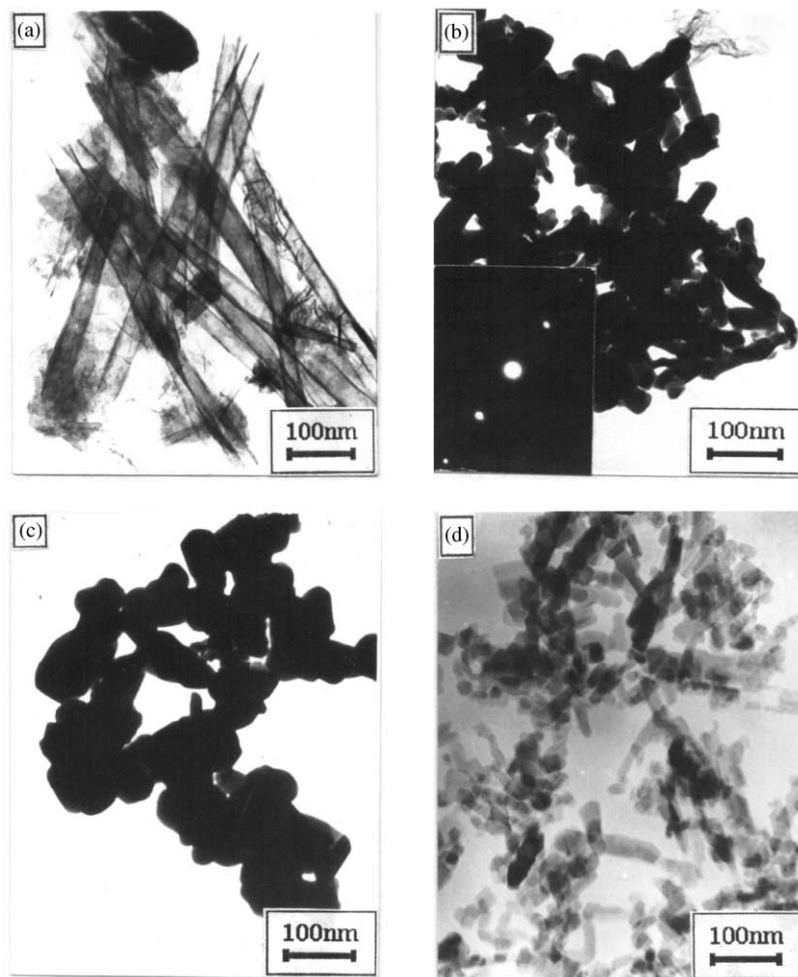
FIG. 3. TEM images of the samples as prepared: (a) $Cu_{2-x}Se$ nanotubes, (b) Cu_2Te nanorods and its SAED pattern (inset in b), (c) Ag_2Se nanoparticles, and (d) Ag_2Te short nanorods.

from the eight stronger peaks, agree well with the literature data (JCPDS 24-1041). The XPS spectra of Ag_2Se (Fig. 2b) shows that the binding energies of $Ag3d5$ and $Se3d$ are 367.85 and 53.25 eV, respectively. The molar ratio of Ag to Se according to the quantification of peaks is 2.000:1.064, close to the stoichiometry of Ag_2Se. Figure 1d shows the XRD pattern of Ag_2Te sample as obtained, which could be indexed as a monoclinic phase. The calculated cell constants shown in Table 1 are consistent with the literature data (JCPDS 34-142). XPS analysis showed a molar ratio of Ag to Te of 2.000:1.047, close to the stoichiometry of Ag_2Te.

The room-temperature reaction of AgCl with Se or Te in the mixed solvent produced nanocrystalline silver selenide and telluride in good yield, respectively. Compared to the synthesis of copper chalcogenides, the synthesis reaction times of Ag_2Se and Ag_2Te were obviously shorter, which may be attributed to the higher activity of the silver cations. In the alkaline mixed solvent, the disproportionation of Se or Te occurred and produced Se^{2-} or Te^{2-} ions (25, 26), while AgCl could be dissolved slowly to form Ag^+, which was then chelated with ethylenediamine to form a stable complex $[Ag(en)_2]^+$. At last, the complex $[Ag(en)_2]^+$ combined with Se^{2-} or Te^{2-} to form nanocrystalline silver chalcogenides. The redox reactions could be illustrated as follows:

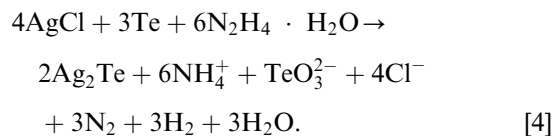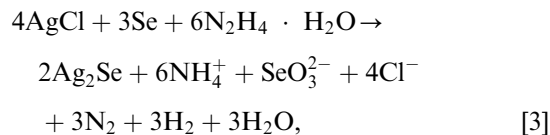$$4AgCl + 3Se + 6N_2H_4 \cdot H_2O \rightarrow$$
$$2Ag_2Se + 6NH_4^+ + SeO_3^{2-} + 4Cl^-$$
$$+ 3N_2 + 3H_2 + 3H_2O, \qquad [3]$$

$$4AgCl + 3Te + 6N_2H_4 \cdot H_2O \rightarrow$$
$$2Ag_2Te + 6NH_4^+ + TeO_3^{2-} + 4Cl^-$$
$$+ 3N_2 + 3H_2 + 3H_2O. \qquad [4]$$

TABLE 2
Effect of Reaction Condition on the Products

Starting materials	Solvent volume ratio en/hydrazine	Reaction time (h)	Products	Morphology
CuO + Se	0	24	CuO + Se + CuSe	Particle
CuO + Se	1:1	24	$Cu_{2-x}Se$	Lamellar + nanotube
CuO + Se	2:1	24	$Cu_{2-x}Se$	Nanotube + lamellar
CuO + Te	0	24	CuO + Te + CuTe	Particle
CuO + Te	1:1	24	Cu_2Te	Nanoparticle + nanorod
CuO + Te	2:1	24	Cu_2Te	Nanorod + nanoparticle
AgCl + Se	0	8	$AgCl + Se + Ag_2Se$	Particle
AgCl + Se	1:1	8	Ag_2Se	Particle
AgCl + Se	2:1	8	Ag_2Se	Particle
AgCl + Te	0	8	$AgCl + Te + Ag_2Te$	Particle
AgCl + Te	1:1	8	Ag_2Te	Nanorod + nanoparticle
AgCl + Te	2:1	8	Ag_2Te	Nanorod

Because of the higher activity of Ag^+ and the low stability of the complex $[Ag(en)_2]^+$ ($\beta_2 = 10^{7.7} M^{-2}$) compared with $[Cu(en)_2]^{2+}$, the nucleation and growth rate of Ag_2Se are faster than that of copper chalcogenides. It is difficult to obtain the small-size nanocrystalline and one-dimensional structure products although the complex $[Ag(en)_2]^+$ is present. The TEM image (Fig. 3c) shows that Ag_2Se is formed as long nanoparticles with a dimension of $40 \times 100 nm^2$. Unlike Ag_2Se, the morphology of Ag_2Te is short nanorods with an average length of 50 nm and a diameter of 10 nm as shown in Fig. 3d, which is similar to that of Cu_2Te. We speculate that because of lower activities of Te^{2-}, the molecular template and the complex $[Ag(en)_2]^+$ might affect the growth of nanocrystalline Ag_2Te.

In order to investigate the influence of the solvent, various solvents with different volume ratios of hydrazine hydrate to ethylenediamine were used respectively, as listed in Table 2, and other reaction conditions were kept constant. When only ethylenediamine was selected, a great deal of unreacted starting materials remained due to their poor solubility in solvent and lack of higher reaction energy barrier hydrazine hydrate. For copper chalcogenides, CuSe and CuTe were found in this case, which might confirm the reductive effect of hydrazine hydrate on the $Cu_{2-x}Se$ and Cu_2Te synthesis reaction. For the room-temperature synthesis reactions, at least 24 h were necessary to form pure phase of copper chalcogenides, $Cu_{2-x}Se$ and Cu_2Te, in the mixed solvents. Because of the higher activity of Ag^+ ions and the lower stability of the complex $[Ag(en)_2]^+$, pure phase of silver chalcogenides, Ag_2Se and Ag_2Te were obtained only in 8 h.

From Fig. 1, the phenomena of diffraction peak broadening could be observed obviously in all XRD patterns. The average grain sizes of the products estimated from Debye–Sherre formula shown in Table 1 are nearer to radial sizes than to axis sizes of all but Ag_2Se nanocrystals. To expect the nanocrystals optical properties, the ultraviolet absorption spectra were measured using anhydrous ethanol as the media. Typical UV-Vis absorption patterns of $Cu_{2-x}Se$ nanotube and Ag_2Te short nanorod are shown in Fig. 4a and 4b, respectively. For Ag_2Te nanocrystals, we found a broad shoulder at 420 nm, indicating that the band-gap energy (E_g) of Ag_2Te nanocrystals was about 2.95 eV, which was much larger than that of the bulk crystal (0.17 eV). For $Cu_{2-x}Se$ nanotube, an absorption shoulder was at 280 nm, indicating a band-gap energy of 4.43 eV, also larger than that of bulk crystal (about 3.0 eV). A further weaker shoulder appeared at 350 nm (3.54 eV), which might be caused by vacancy defects in the mixed valence state compound. These obvious blueshifts might be caused by nanosize effects and structure defects of nanocrystals (29, 30). Similar broad absorption phenomena were also observed in Cu_2Te and Ag_2Se nanocrystals.
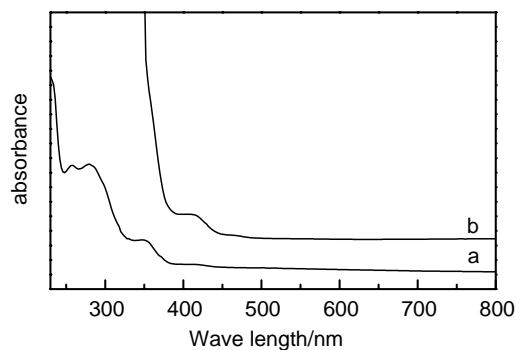

FIG. 4. UV-Vis absorption spectra: (a) $Cu_{2-x}Se$ nanotubes and (b) Ag_2Te short nanorods.

IV. CONCLUSIONS

Copper and silver nanocrystalline chalcogenides, $Cu_{2-x}Se$, Cu_2Te, Ag_2Se, and Ag_2Te with different morphologies such as nanotubes, short nanorods, and nanoparticles have been successfully synthesized in the mixture of ethylenediamine and hydrazine hydrate as a solvent at room temperature. The coordinating and chelation abilities of ethylenediamine play an important role in the formation of one-dimensional nanocrystalline binary chalcogenides. Hydrazine hydrate is crucial to the electron transfer in the redox reactions. Pure $Cu_{2-x}Se$, Cu_2Te, Ag_2Se, and Ag_2Te could be obtained in the mixed solvent with the volume ratio of en to hydrazine hydrate in the range from 2 to 3 at 24 h for copper chalcogenides and 8 h for silver chalcogenides. It is reasonable that this convenient room-temperature reaction could be used to synthesize other transition metal selenides and tellurides in nanocrystalline form. The UV-Vis absorption spectra showed some new characteristics of these nanocrystals. Further studies are needed to investigate the effect and mechanism of broad absorption with blueshift.

ACKNOWLEDGMENTS

REFERENCES

1. M. G. Bawendi, D. J. Carroll, W. L. Wilson, and L. E. Brus. *J. Chem. Phys.* **96,** 946 (1992).
2. B. P. Zhang, T. Yasuda, Y. Segawa, H. Yaguchi, K. Onabe, E. Edamatsu, and T. Itoh, *Appl. Phys. Lett.* **70**(18), 2413 (1997).
3. W. Z. Wang, Y. Geng, P. Yan, F. Y. Liu, Y. Xie, and Y. T. Qian, *J. Am. Chem. Soc.* **121,** 4062 (1999).
4. Y. Li, Y. Ding, Y. T. Qian, Y. Zhang, and L. Yang, *Inorg. Chem.* **37,** 2844 (1998).
5. T. Chivers, *J. Chem. Soc., Dalton Trans.* 1185 (1996).
6. J. J. Ritter and M. Pichai, *Inorg. Chem.* **34**(16), 4278 (1995).
7. H. Toyoji and H. Yao, *Jpn. Kokai Tokkyo Koho Jp02* **173,** 622.
8. F. Mongellaz, A. Fillot, and J. De Lallee, *Proc. SPIE-Int. Soc. Opt. Eng.* **156,** 2227 (1994).
9. S. T. Lakshmikvmar, *Sol. Energy Mater. Sol. Cell* **32,** 7 (1994).
10. A. A. Korzhuev, *Fiz. Khim. Obrab. Mater.* **3,** 131 (1993).
11. H. S. Schnyders and M.-L. Saboungi, *Appl. Phys. Lett.* **76**(13), 1710 (2000).
12. R. Xu, A. Husmann, T. F. Rosenbaum, M.-L. Saboungi, J. E. Enderby, and P. B. Littlewood, *Nature* **390,** 57 (1997).
13. R. Coustal, *J. Chem. Phys.* **38,** 277 (1958).
14. H. C. Yi and J. J. Moore, *J. Mater. Sci.* **25,** 1159 (1990).
15. I. P. Parkin, *Chem. Soc. Rev.* **25,** 199 (1996).
16. H. C. Metcalf, J. E. Williams, and J. F. Caskta, "Modern Chemistry," p. 54. Holt, Reinhart, Winston, New York, 1982.
17. G. Henshaw, I. P. Parkin, and G. Shaw, *J. Chem. Soc. Chem. Commun.* 1095 (1996).
18. G. Henshaw, I. P. Parkin, and G. Shaw, *J. Chem. Soc. Dalton. Trans.* 231 (1997).
19. W. Z. Wang, P. Yan, F. Y. Liu, Y. Xie, Y. Geng, and Y. T. Qian, *J. Mater. Chem.* **8**(11), 2321 (1998).
20. S. H. Yu, Z. H. Han, J. Yang, R. Y. Yang, Y. Xie, and Y. T. Qian, *Chem. Lett.* (1998).
21. R. Tenne, M. Homyonfer, and Y. Feldman, *Chem. Mater.* **10,** 3225 (1998).
22. M. Homyonfer, B. Alperson, Y. Rosenberg, L. Sapir, S. R. Cohen, G. Hodes, and R. Tenne, *J. Am. Chem. Soc.* **119,** 2693 (1997).
23. C. D. Wanger, W. M. Riggs, L. E. Davis, and J. F. Moulder, *in* "Handbook of X-ray Photoelectron Spectroscope," (G. E. Muilenberg, Ed.), pp. 82–83. Perkin-Elemer Corporation, Minnesota, 1979.
24. D. Briggs and M. P. Seah, *in* "Practical Surface Analysis by Auger and X-ray Spractroscopy," (Ed.), p. 496. John Wiley & Sons: New York, 1983.
25. E. Best, I. Hinz, and H. Wendt, *in* "Gmelin Handbuch der Anorganischen Cemie, Se," pp. 149–150. Springer-Verlag, Berlin, Heidelberg, New York, 1979.
26. E. Best, U. T. Raußendorf, and J. Wanger, *in* "Gemlin Handbook of Inorganic Chemistry, Te" (G. Kirschstein, Ed.), pp. 22–23. Springer, Berlin, Heidelberg, New York, 1982.
27. M. E. Spahr, P. Bitterli, R. Nesper, M. Müller, F. Krumeich, and H. U. Nissen, *Angew. Chem. Int. Ed.* **37,** 1263 (1998).
28. F. Krumeich, H. J. Muhr, M. Niederberger, F. Bieri, B. Schnyder, and R. Nesper, *J. Am. Chem. Soc.* **121,** 8324 (1999).
29. L. E. Brus, *J. Phys. Chem.* **80,** 142 (1985).
30. L. E. Brus, *J. Phys. Chem.* **89,** 2555 (1986).